

Properties of Action-Potential Initiation in Neocortical Pyramidal Cells: Evidence From Whole Cell Axon Recordings

Youzheng Shu, Alvaro Duque,* Yuguo Yu,* Bilal Haider, and David A. McCormick

Department of Neurobiology, Kavli Institute for Neuroscience, Yale University School of Medicine, New Haven, Connecticut

Submitted 30 August 2006; accepted in final form 2 November 2006

Shu Y, Duque A, Yu Y, Haider B, McCormick DA. Properties of action-potential initiation in neocortical pyramidal cells: evidence from whole cell axon recordings. *J Neurophysiol* 97: 746–760, 2007; First published November 8, 2006; doi:10.1152/jn.00922.2006. Cortical pyramidal cells are constantly bombarded by synaptic activity, much of which arises from other cortical neurons, both in normal conditions and during epileptic seizures. The action potentials generated by barrages of synaptic activity may exhibit a variable site of origin. Here we performed simultaneous whole cell recordings from the soma and axon or soma and apical dendrite of layer 5 pyramidal neurons during normal recurrent network activity (up states), the intrasomatic or intradendritic injection of artificial synaptic barrages, and during epileptiform discharges in vitro. We demonstrate that under all of these conditions, the real or artificial synaptic bombardments propagate through the dendrosomatic-axonal arbor and consistently initiate action potentials in the axon initial segment that then propagate to other parts of the cell. Action potentials recorded intracellularly in vivo during up states and in response to visual stimulation exhibit properties indicating that they are typically initiated in the axon. Intracortical axons were particularly well suited to faithfully follow the generation of action potentials by the axon initial segment. Action-potential generation was more reliable in the distal axon than at the soma during epileptiform activity. These results indicate that the axon is the preferred site of action-potential initiation in cortical pyramidal cells, both in vivo and in vitro, with state-dependent back propagation through the somatic and dendritic compartments.

INTRODUCTION

Cortical pyramidal cells have several active zones that are independently capable of generating action potentials. These include at least the apical and basal dendrites, soma, axon hillock, axon initial segment, and more distal components of the axon, such as the nodes of Ranvier (Colbert and Johnston 1996; Colbert and Pan 2002; Mainen et al. 1995; Milojkovic et al. 2005; Stuart et al. 1997a,b). Which compartment is the first to initiate action potentials and how far these spikes propagate and interact with the other compartments may have a significant effect on short- and long-term cortical function (Golding et al. 2002; Larkum et al. 1999a; Svoboda et al. 1997; Waters and Helmchen 2004). In addition, the different compartments of cortical neurons may interact to generate complex patterns of spike generation, such as burst discharges, prolonged depolarizations, and oscillations (Helmchen et al. 1999; Kim and Connors 1993; Larkum and Zhu 2002; Larkum et al. 2001; Stuart et al. 1997b; Wang 1999).

Investigations of even low-frequency single-spike initiation (the simplest form of action-potential generation) in cortical

pyramidal cells have yielded some conflicting results, although the general consensus is that in response to somatic depolarizing current pulses or local, electrical activation of threshold synaptic inputs, fast spikes are initiated in the axon initial segment followed by back propagation into the soma and apical dendrite (Palmer and Stuart 2006; Stuart et al. 1997a,b). This finding is in agreement with classical studies in spinal motoneurons (Coombs et al. 1957; Fuortes et al. 1957), although some studies have suggested that the first node of Ranvier, and not the axon initial segment, is the typical site of action-potential initiation in some cell types (Clark et al. 2005; Colbert and Johnston 1996; Colbert and Pan 2002).

Although these studies indicate that the axon initial segment is the preferred site of spike initiation under the relatively quiescent conditions of the in vitro slice, the site of fast spike initiation under conditions when the cortical network is active is still relatively unexplored. In vivo, cortical pyramidal neurons receive tens of thousands of synaptic inputs, which often culminate in prolonged depolarizations and significant increases in membrane conductances of both dendritic and somatic compartments (Destexhe et al. 2001; Steriade et al. 2001). One example of complex barrages of synaptic activity is the up state of the slow oscillation that occurs during slow wave sleep or anesthesia (Haider et al. 2006; Steriade et al. 1993, 2001). The synaptic barrages arriving during the up state display properties that are similar, but not identical, to those of the waking state (Steriade et al. 2001). The properties of fast spike initiation in cortical pyramidal cells during ongoing barrages of synaptic activity, and how these give rise to spike threshold variability (Azouz and Gray 1999), are not well understood. Simultaneous dendritic and somatic extracellular recordings in vivo indicate that action potentials are typically back-propagating from the soma into the apical dendrites, although the precise location of initiation of these spikes could not be discerned (Buzsaki and Kandel 1998). Simultaneous in vivo dendritic Ca^{2+} imaging and somatic recordings suggest that layer 2/3 pyramidal cells may generate apical dendritic spikes only after somatic spikes (Svoboda et al. 1997, 1999), whereas the apical dendrites of layer 5 pyramidal neurons may occasionally generate Ca^{2+} transients (presumed action potentials) in isolation of somatic spikes (Helmchen et al. 1999). Indeed, in vitro studies have suggested that action potentials may initiate first from dendritic compartments during strong and/or synchronous synaptic stimulation to localized or distributed portions of the dendritic tree (Gasparini et al. 2004; Golding and Spruston 1998; Larkum et al. 1999a,b; Losonczy

* A. Duque and Y. Yu contributed equally to this work.

Address for reprint requests and other correspondence: D. A. McCormick, Dept. of Neurobiology, Yale University School of Medicine, 333 Cedar St., New Haven, CT 06510 (E-mail: david.mccormick@yale.edu).

The costs of publication of this article were defrayed in part by the payment of page charges. The article must therefore be hereby marked “advertisement” in accordance with 18 U.S.C. Section 1734 solely to indicate this fact.

and Magee 2006; Milojkovic et al. 2005; Regehr et al. 1993; Schiller et al. 1997), and these dendritic spikes may or may not propagate completely to the soma (Jarsky et al. 2005; Larkum and Zhu 2002; Larkum et al. 2001; Losonczy and Magee 2006; Milojkovic et al. 2005; Schiller et al. 1997). Dendritic and somatic interactions are even more complex during the generation of bursts of action potentials, in which rapid action potentials may be initiated in the axonal/somatic compartments, whereas the generation of slower spikes or other active depolarizing events in the dendrites provide the prolonged depolarization that drives the burst (Helmchen et al. 1999; Kim and Connors 1993; Larkum and Zhu 2002; Larkum et al. 2001; Stuart et al. 1997b; Wang 1999).

These results suggest that the site of spike initiation in regular spiking cortical pyramidal cells may vary according to the nature of the initiating stimulus, with threshold stimuli preferring initiation in the axon (initial segment or 1st node of Ranvier) and strong, synchronized, or distal stimuli occasionally initiating spikes from the dendrites. Given the possibility of spikes being initiated in variable portions of the neuron, it is not clear where these action potentials will be initiated under the various conditions occurring *in vivo*, including during ongoing synaptic barrages (either spontaneous or evoked by sensory stimuli), or under pathological conditions, such as during epileptic seizures. Here, as a first step toward investigating this question, we examine the properties of spike initiation in cortical pyramidal cells during the spontaneous generation of up states *in vitro* and *in vivo*, in response to sensory stimuli *in vivo*, during epileptiform discharges *in vitro*, and during the intradendritic and intrasomatic injection of complex patterns of current *in vitro*. We provide evidence that under all of these conditions, fast action potentials are preferentially initiated from the axonal initial segment and propagate reliably down the axon.

METHODS

Experiments were performed on 0.3-mm thick slices of the ferret (7–10 wk old) prefrontal cortex (anterior to the Sylvian fissure) but also from somatosensory area and maintained *in vitro* in a submerged style recording chamber at 36.5°C. Immediately after cutting, the slices were transferred to an incubation beaker filled with aerated normal artificial cerebrospinal fluid (ACSF) containing (in mM) 126 NaCl, 2.5 KCl, 2 MgSO₄, 2 CaCl₂, 26 NaHCO₃, 1.25 NaH₂PO₄, and 25 dextrose (315 mosM, pH 7.4) and held at 35°C until use. After ≥1 h of incubation, slices were transferred to a submerged chamber in which both a bottom and top grid were used to lift and hold the slices in position and that contained the ACSF solution as in the preceding text. Cortical neurons were visualized with an upright infrared-differential interference contrast (IR-DIC) microscope (Zeiss Axioskop 2 FS plus). A light-sensitive camera (OLY-150, Olympus) was used for tracing the fluorescent axonal profiles. For only those recordings where the slow oscillation or epileptic activity was examined in the submerged chamber, the ACSF solution was modified to contain (in mM) 1 MgSO₄, 1 CaCl₂, and 3.5 KCl (Sanchez-Vives and McCormick 2000; Shu et al. 2003a,b). The membrane potentials in our whole cell recordings were not corrected for Donnan liquid junction potential, which is between 5 and 15 mV (Fricker et al. 1999).

Whole cell recordings were achieved simultaneously from either the soma and the apical dendrite or the soma and the cut end of the main axon using a Multiclamp 700B or Axoclamp 2B amplifier (Molecular Devices, Sunnyvale, CA). Patch pipettes were formed on a Sutter Instruments (Novato, CA) P-97 microelectrode puller from

borosilicate glass (1B200-4, WPI, Sarasota, FL). Pipettes for somatic recording had an impedance of 5–6 MΩ and were filled with an intracellular solution that contained (in mM) 140 KGluconate, 3 KCl, 2 MgCl₂, 2 Na₂ATP, and 10 HEPES, pH 7.2 with KOH (288 mosM). Calcium buffer included in the whole cell pipette was 0.2 mM EGTA. Only regular spiking neurons were analyzed in this study.

Alexa Fluor 488 (100 μM) and biocytin (0.2%) were added to the pipette solution for tracing and labeling the recorded pyramidal cells. For simultaneous somatic and axonal (prefrontal cortex) or somatic and dendritic (typically in somatosensory cortex) whole cell recordings, ~10 min after somatic whole cell recording was established, the course of the main axon or apical dendrite was examined under the fluorescent microscope equipped with a ×40 water-immersion objective and a magnifier of up to ×2. Only those pyramidal neurons in which the apical dendrite or axon was preserved and came to the upper surface of the slice were used in this portion of our study. Patch pipettes for whole cell dendritic or axonal recording were filled with a similar intracellular solution but without fluorescent dye added; these had an impedance of 9–15 MΩ. The pipette was advanced to the apical dendrite or the cut end of the axon with a positive pressure of ~65 mbar and guided by switching back and forth between the fluorescent and DIC images with the total time the cell was exposed to fluorescence being kept to <20 s to minimize damage (our whole cell recordings from the soma did not reveal any evidence of changes in the electrophysiological properties of the recorded neurons during this brief exposure to fluorescence). The apical dendrite or the bleb formed at the cut end of the axon was then pressed by the pipette tip and negative pressure was applied to form a seal. As soon as a tight seal (>10 GΩ) was achieved, pulses of brief suction were applied to break the patch, and the whole cell configuration could be easily obtained. Thereafter steps of positive and negative current were injected to the soma to examine the intrinsic membrane properties of the recorded neuron. During the whole period of simultaneous somatic and dendritic, or somatic and axonal recordings, access resistance was monitored frequently; recordings with access resistance >25 MΩ for somatic recording, 80 MΩ for axonal or dendritic recording, were discarded. Bridge balance and capacitance neutralization were carefully adjusted before and after every experimental protocol. After a recording was completed, the slice was transferred to 4% paraformaldehyde in 0.1 M phosphate buffer for subsequent immunostaining and visualization.

All computations were performed in Spike2 (Cambridge Electronic Design, Cambridge, UK) and MATLAB (MathWorks, Bethesda, MD). All error bars were calculated as the mean ± SE, and data in the text are reported as means ± SD.

A number of experiments were performed with a dynamic-clamp technique using a DAP-5216a board (Microstar Laboratory). Noisy conductances were constructed according to an Ornstein-Uhlenbeck (colored noise) model (Destexhe et al. 2001). The SD (and, concurrently, the amplitude) of the conductance was adjusted to give a 10-mV peak-to-peak membrane potential deviation, and the holding current was adjusted to keep the cell just near spike threshold.

The *in vivo* intracellular recordings analyzed here were from previously published studies performed in the primary visual cortex of halothane anesthetized cats (Nowak et al. 2005) or ketamine-xylazine-anesthetized ferrets (Haider et al. 2006). Analysis was restricted to those neurons classified as regular spiking, according to standard criteria (McCormick et al. 1985; Nowak et al. 2003).

Anatomical methods

Male ferrets, 7-wk or 15-mo old, were used for examination of the axon region of myelination, mainly in the ferret prefrontal cortex.

MYELIN STAINING

BULK SILVER STAINING. Because silver staining can make visible even the thinnest fibers of myelin in the cortex and it has been

successfully used in various animal species, to visualize the overall pattern of myelination in the ferret brain, we used a modified version of the silver staining of myelin technique described by Gallyas (1979) using 40- μm -thick, formalin fixed, vibratome cut brain sections mounted on gelatin subbed glass slides (Fig. 5A).

SINGLE AXON IMMUNOHISTOCHEMISTRY. To visualize myelin in single axons (Fig. 5, C and D), layer 5 pyramidal cells in the ferret prefrontal cortex were intracellularly injected (in vitro, 300- μm -thick sections as used for recordings) with 0.2% biocytin and immersion fixed in 4% paraformaldehyde. After rinsing with 0.1 M PB, sections were permeabilized in 50% cold methanol in 0.1 M PB containing 3% hydrogen peroxide and 0.5% triton X (45', RT). Sections were then incubated in anti-myelin basic protein (Mouse anti SMI-94, 1:1000 in 0.1 M PB, 2 nights at 4°C; Sternberger Monoclonals, Covance Research Products, Berkeley, CA) and developed with a combination of Avidin conjugated Alexa-488 and CY-5 conjugated goat anti-mouse secondary antibody (both at 1:500 in 0.1 M PB, overnight; Jackson ImmunoResearch Laboratories, West Grove, PA).

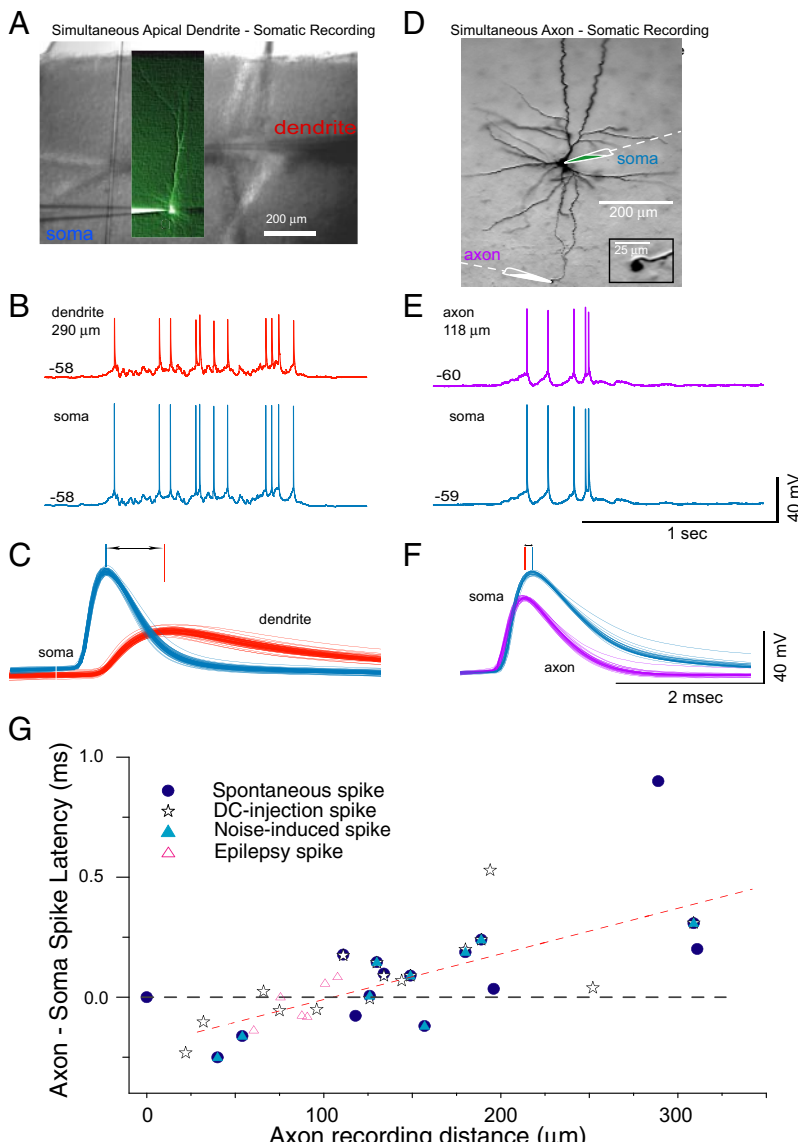
GOLGI STAINING. For Golgi staining (Fig. 5B, supplemental Fig. 2), we used a commercially available kit that has combined and improved the Golgi-Cox and the classical rapid Golgi methods. This kit, known as the FD Rapid GolgiStain (FD NeuroTechnologies, Ellicott City,

MD) is convenient to use because it is highly reliable and results in excellent staining of unmyelinated axons while preserving staining of somata and dendritic spines. Also, this method works well in older specimens, an important feature since a commonly cited drawback of Golgi impregnation is that it has been sometimes observed to work well only in young animals (Millhouse 1981).

MICROSCOPY AND DOCUMENTATION. Bulk silver staining of myelin and Golgi preparations were observed under a Zeiss Axiphoto microscope. Digital images were acquired with an AxioCam HRc camera and Axiovision software. Single stained axons double-labeled for myelin using immunohistochemistry were observed using a Zeiss LSM 510 Meta confocal microscope system direct-coupled to a Zeiss Axiovert 100M microscope. Digital photos were minimally manipulated for contrast and brightness in Adobe Photoshop. Drawings and illustrations were made in Adobe Illustrator.

Model methods

Our computational model (Fig. 6) was implemented using NEURON 5.8 (Hines and Carnevale 1997) and was based on the multi-compartmental model of the full dendritic and somatic structure of a layer 5 cortical pyramidal cell (Fig. 1D in Mainen and Sejnowski



1996) coupled with a reconstruction of cortical pyramidal cell axons according to Binzegger et al. (2005). We used this model recently to examine the passive propagation properties of intracortical axons (Shu et al. 2006). The temperature of the modeled cell was 37°C.

DENDRITES AND SOMA. The soma and dendrites contain 164 segments. The somatic surface area is 2,748 μm^2 , whereas its diameter is 25 μm and its length is 35 μm . There are 11 primary neurites, 87 branches, totaling 17,668 μm in length and 78,858 μm^2 in surface area.

AXON. Our model of the axon began with that of Mainen et al. (1995) and was subsequently modified to include either a reduced axonal arbor that was of similar length and branching pattern as that of our biocytin-filled neurons *in vitro* or a more complete axonal arbor modeled after that of Binzegger et al. (2005). In addition, we modified membrane capacitance and ionic conductances to match the spike initiation properties of our layer 5 pyramidal cells (McCormick, Shu, and Yu, unpublished results).

MAIN AXON. The soma connects to the axon hillock, which tapers from 2.4 to 0.92 μm and has a length of 10 μm . The hillock is followed by a 40- μm initial segment of 0.92 μm diam. After the initial segment, there is a 300- μm length of unmyelinated axon (0.55 μm in diameter) based on our examinations on the main axons of prefrontal cortical neurons in 7-wk-old ferrets. For modeling the full axonal arbor, the next portion of the main axon is myelinated and 3,000 μm in length with internode distances of 200 μm . The diameter of the internodal axon is 0.92 μm . The diameter of axonal nodes is 0.46 μm , and their length is 1 μm .

AXON COLLATERALS OF FULL LAYER 5 PYRAMIDAL CELL. All collaterals were assumed to be unmyelinated (Shu et al. 2006). There are eight first-order collaterals (diameter: 0.46 μm), 23 second-order collaterals (diameter: 0.37 μm), and 131 third-, fourth-, and fifth-order collaterals (diameter: 0.37 μm). The total length of collaterals is \sim 64 mm. Including the main axon, the total axon length is 66.7 mm.

AXON COLLATERALS OF "SLICE" LAYER 5 PYRAMIDAL CELL. For the slice neuron simulation, the dendritic tree and soma are the same as in the simulated full neuron, but there are six first-order collaterals, 22 second-order collaterals, totaling 18.7 mm in length consisting of 35 sections composed of 3,293 compartments. With the main axon, the total axonal length for the slice neuron is 19.2 mm.

ELECTRICAL PROPERTIES. The membrane capacitance C_m for the soma, dendrites, unmyelinated axon, and axon collaterals is modeled as 0.7 $\mu\text{F}/\text{cm}^2$, whereas for myelinated axon it is 0.04 $\mu\text{F}/\text{cm}^2$. The axial resistance for dendrite and axon is 100 Ωm (Mainen and Sejnowski 1996). The membrane time constant of the soma, dendrite, hillock and initial segment is 21 ms, whereas for the main axon and collaterals the time constant ranges from 2 to 10.5 ms.

CHANNEL DISTRIBUTIONS. The transient Na^+ current is present in all parts of the modeled cell and its density is high in the initial segment, hillock, and node (7,500 $\text{pS}/\mu\text{m}^2$) but lower in the soma (750 $\text{pS}/\mu\text{m}^2$) and dendrites (20 $\text{pS}/\mu\text{m}^2$). In unmyelinated model axon and collaterals, Na^+ conductance is between 750 and 2,500 $\text{pS}/\mu\text{m}^2$ (the thinner the collateral, the lower the value of the Na^+ conductance). The density of Na^+ conductance was low (20 $\text{pS}/\mu\text{m}^2$) in the myelinated portions of the axon. The reversal potential of Na^+ in our model is 60 mV. The fast, voltage activated K^+ current, I_{Kv} is present in the model hillock, initial segment, and node (1,000 $\text{pS}/\mu\text{m}^2$). The density is lower for soma (400 $\text{pS}/\mu\text{m}^2$), unmyelinated model axon (500 $\text{pS}/\mu\text{m}^2$), and axon collaterals (200 $\text{pS}/\mu\text{m}^2$ for 1st-order collaterals, 100 $\text{pS}/\mu\text{m}^2$ for higher-order collaterals). The reversal potential of K^+ is -90 mV.

The slow noninactivating potassium current (M-current; I_{Km}), high-voltage activated Ca^{2+} current, I_{Ca} and one Ca^{2+} -dependent K^+

current, I_{KCa} , are distributed throughout the soma and dendrites (K_m conductance 0.1, Ca conductance 0.3, and K_{ca} conductance is 3 $\text{pS}/\mu\text{m}^2$) as per Mainen et al. (Mainen and Sejnowski 1996). The reversal potential of Ca is 140 mV. Background leak current is distributed throughout the cell. In the soma, dendrites, hillock, initial segment, and myelinated axon, $g_{\text{leak}} = 0.0000333 \text{ S}/\text{cm}^2$. In the unmyelinated axon and collaterals, $g_{\text{leak}} = 0.00006667 \text{ S}/\text{cm}^2$. In the nodes, $g_{\text{leak}} = 0.02 \text{ S}/\text{cm}^2$. The value of the leak conductance is modified to give time constants that are similar to what we observed in experiments. The reversal potential of the leak current is -70 mV. For the specific rate functions for the different ionic channels, see Mainen and Sejnowski (1996).

RESULTS

In cortical slices, the main axon of pyramidal cells travels to the surface of the slice where it forms a patchable (Shu et al. 2006) spherical 3–6 μm bleb owing to being cut during the slice procedure (Fig. 1*D*). Here we perform whole cell recordings from the axon, apical dendrite, and soma to examine the properties of action-potential generation in layer 5 cortical regular spiking pyramidal cells in the prefrontal cortex in response to current injections and during spontaneous synaptic activity of the up state (Shu et al. 2003b, 2006) as well as during epileptiform discharges. We then compare our results with action potentials recorded *in vivo* during up states and in response to visual stimulation.

Whole cell recordings were obtained simultaneously from either the cell body and apical dendrite ($n = 7$) or cell body and axon ($n = 16$) of cortical pyramidal cells during spontaneous up and down states in ferret prefrontal or somatosensory cortical slices maintained *in vitro* (Fig. 1). These up states are characterized by 5- to 15-mV amplitude, 0.25- to 1-s duration barrages of synaptic activity containing approximately an equal mixture of excitatory and inhibitory potentials (Fig. 1, *B* and *E*) (Haider et al. 2006; Shu et al. 2003b). This synaptic activity arises from the discharge of neighboring neurons and results in the activation of action potentials in the soma at the rate of 5–31 Hz (10–90th percentiles) with an average discharge rate of 11.2 ± 3.2 (SD) Hz ($n = 7$; supplementary Fig. 1*A*¹).

Simultaneous recordings from pyramidal somata and apical dendrites (50–580 μm from the soma) during the generation of spontaneous up states revealed that action potentials were generated in both the cell body and apical dendrite. Examination of the timing of these action potentials revealed that all action potentials were generated in the soma prior to the apical dendrite ($n = 637$ spikes in 7 neurons; Fig. 1*C*) even at all frequencies of action-potential generation from 5 to 75 Hz. The dendritic action potentials decreased in amplitude and broadened in duration with increases in distance from the cell body (not shown). Consistent with previous findings, these recordings revealed that action potentials propagate from the soma up the apical dendrite at a speed of $0.66 \pm 0.18 \text{ m/s}$ ($n = 6$) (Larkum et al. 2001; Stuart et al. 1997a).

Simultaneous recordings from the axon and soma of pyramidal cells during the spontaneous generation of up states revealed a spike timing relationship that varied with the distance of the axonal recording site from the soma ($n = 16$). Recordings in which action potentials arrived at the axonal recording site prior to the soma were obtained at axonal

¹The online version of this article contains supplemental data.

distances of between 40 and 157 μm (Fig. 1, *D–G*), whereas axonal recordings that exhibited spikes occurring after those in the soma were recorded at distances of 111–311 μm (see following text; Fig. 1*G*). Plotting the time difference between the axonal and somatic spike times versus location of the axonal recording site revealed a relationship that fell to zero difference at a distance of ~ 80 – $110 \mu\text{m}$ (Fig. 1*G*). If the action potentials were to propagate orthodromically and antidromically from their site of origin with equal speed, then spikes that arrive at the same time at the axonal and somatic recording sites are likely to have initiated at a point halfway between the two. Therefore these results suggest that during spontaneous up states, action potentials are initiated in the axon somewhere between 40 and 55 μm from the soma. Our computational model suggests, however, that action potentials propagate orthodromically away from their site of origin at an average speed of 0.83 m/s, whereas they propagate antidromically toward the cell body at an average speed of 0.7 m/s (see Fig. 6). These simulations suggest that our present method of estimation of the site of spike initiation should be compensated by $\sim 10 \mu\text{m}$ toward the soma.

Action potentials initiated by artificial up states

To control the precise location of the arrival of the currents initiating action potentials, we used the dynamic-clamp technique to inject artificial barrages of synaptic activity in the apical dendrite or soma while performing dual dendritic-somatic or somatic-axonal recordings ($n = 10$; Fig. 2). As with naturally occurring barrages of synaptic activity, these artificial barrages resulted in action potentials that occurred first in the soma followed by propagation into the apical dendrite (Fig.

2*A*), at all frequencies of action-potential generation from 2 to 34 Hz (supplementary Fig. 1*B*), for both somatic and apical dendritic injections. The injection of artificial up states into the soma resulted in action potentials, the timing difference of which between the soma and axon (Fig. 2, *C* and *D*) exhibited a zero difference at $\sim 110 \mu\text{m}$ (Fig. 1*G*), indicating that these spikes are initiated at $\sim 55 \mu\text{m}$ from the cell body, in the axon initial segment. Similar results were obtained with action potentials generated in response to current pulses and during epileptiform activity (see Fig. 1*G* and following text).

Responses to current pulse injection

By initiating spikes with the intracellular injection of short-duration current pulses at either the somatic or axonal recording sites and examining the timing relationship of these action potentials versus distance between the recording locations, we were also able to calculate the apparent action-potential initiation site using simple algebra (Fig. 3). Our calculation revealed that in response to somatic current pulses action potentials initiate $\sim 46 \pm 5.6 \mu\text{m}$ ($n = 16$ cells) down the axon from the edge of the soma. This location, however, should be compensated for possible differences in antidromic versus orthodromic conduction velocities in our experiments (see text above).

We investigated the properties of action-potential generation further through the initiation of spikes with the intracellular injection of long duration (100–500 ms) current pulses of 0.1- to 5-nA amplitude, delivered through either the soma or axon whole cell recording electrodes (Fig. 4; $n = 22$ cells). We found that there was a gradation of electrophysiological properties among three active zones: the soma, axon initial segment, and distal axon. The injection of prolonged current

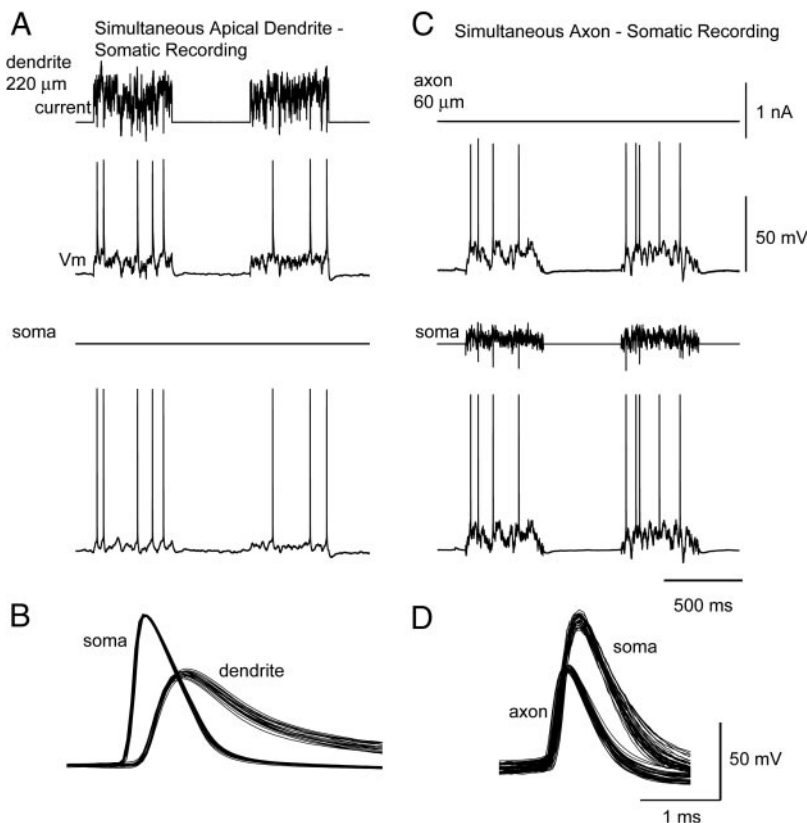


FIG. 2. Action potentials are initiated in the axon initial segment during the injection of network postsynaptic potential (PSP)-like conductances. *A*: simultaneous apical dendritic (220 μm) and somatic whole cell recording during the injection of artificial up states with a dynamic-clamp system into the apical dendrite. *B*: comparing the spikes occurring in the soma and dendrite during artificial up states revealed that they also occurred first in the soma and then back propagated to the dendrite. *C*: simultaneous whole cell recordings from the soma and axon (60 μm distant) during the injection of artificial up states into the soma. *D*: action potentials initiated 1st in the axon and then propagated into the soma.

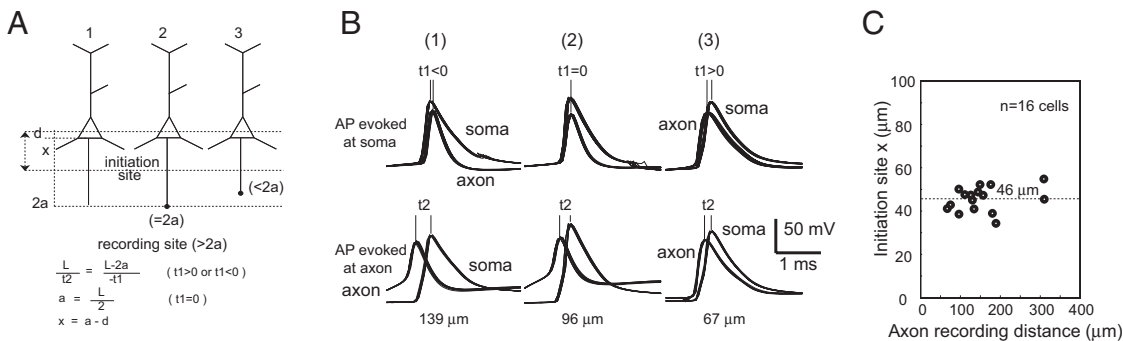


FIG. 3. Calculation of the initiation point of the action potential reveals an origin of $\sim 46 \mu\text{m}$ from the soma. *A*: schematic diagram illustrating the use of simple algebra to calculate the initiation point of action potentials based on the relative timing of spikes initiated with depolarizing current pulses delivered to the soma or to the axon. *a*, distance from the center of the soma to the initiation site; *d*, distance from the center of the soma to the origin of the axon; *x*, distance from the origin of the axon to the initiation site; *L*, distance between the 2 recording sites; *t*₁, latency difference between the axon and somatic recorded action potentials when evoked with a somatic current pulse; *t*₂, latency difference between axon and somatic recorded action potentials when evoked with a current pulse at the end of the axon. *B*: 3 examples of simultaneous whole cell recordings illustrating the 3 possible timing relationships between cell body and axon for spikes initiated in the axon initial segment (*top traces*). Multiple traces from each recording are overlaid. In the 1st example (1), the axonal recording is 139 μm from the cell body, and the spike arrives in the soma 1st (*top traces*). In the 2nd example (2), the axonal recording is 96 μm from the cell body, and the action potential arrives in the soma and axonal recording site at about the same time. In the 3rd example (3), the axonal recording is 67 μm from the cell body, and the action potential arrives at the axonal recording site first. Bottom traces illustrate timing relation when action potentials are initiated at the end of the axon in each paired recording. *C*: plot of the results of the calculation of the initiation site versus the distance from the cell body of the axonal recording. The calculated initiation site is relatively consistent with an average of 46 μm .

pulses into the soma or proximal axon initial segment (22–97 μm from the soma) resulted in the repetitive generation of action potentials in both the somatic and axonal recording sites. Increasing the amplitude of somatic injected current resulted in

an increase in action-potential frequency and a broadening of action-potential duration in both the soma and the axon (Fig. 4, *A–D* and *F*). Action-potential amplitude in both the soma and axon initial segment decreased with large current injections

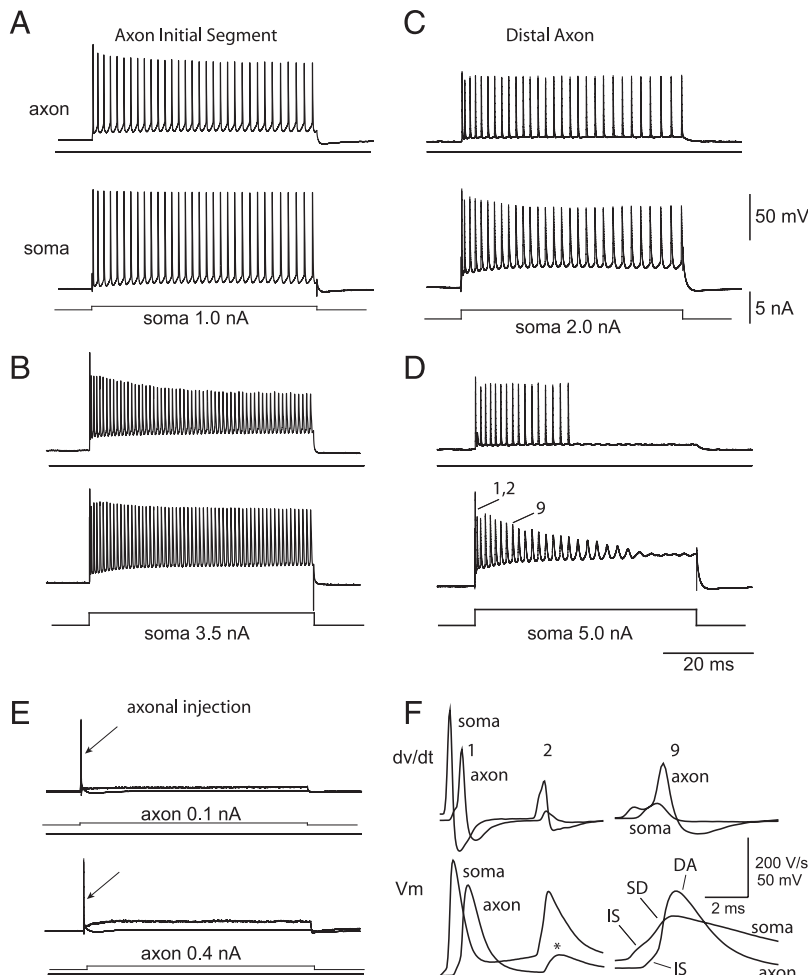


FIG. 4. Responses to the somatic and axonal injection of current pulses. Responses of the axon initial segment (50 μm from the soma) to 1.0 nA (*A*) and 3.5 nA (*B*) of current injection into the soma. Note that with large somatic current injections, the action potentials in both the soma and axon initial segment become smaller in amplitude. *C* and *D*: response of a cell body and distal axon (440 μm , *top trace* in each pair) to moderate (2 nA) and intense somatic current injection (5 nA). Here, the axonal spikes do not decrease markedly in amplitude. *E*: intraxonal (151 μm from the soma) injection of a threshold (0.1) and larger (0.4 nA) current results in the initiation of only a single action potential at the beginning of the pulse. *F*: expanded action potentials and dV/dt (action potentials 1, 2, and 9) as recorded from the soma and distal axon during the intense current pulse of *D*. Note the fractionation of the spikes into components, which presumably are initiated in the initial segment (IS), somatodendritic (SD), and distal axon (DA) regions. *, IS spike that failed to propagate down the axon.

(Fig. 4, *B* and *D*), whereas action-potential amplitude in the distal axon was less susceptible to strong depolarization of the soma (Fig. 4, *C* and *D*). With very large somatic depolarizations (≥ 5 nA), action-potential generation occasionally failed in either the axonal or somatic recording site (Fig. 4*D*). In addition, action potentials were observed to fractionate into components, which were especially pronounced when dV/dt of the action potential was examined (Fig. 4*F*). There appeared to be at least three components to these action potentials. The smallest component, as recorded from the soma or distal axon, preceded spike generation in both the distal axonal and somatic recording sites (Fig. 4*F*). Because of this timing, and the presence of this smaller spike even when action potentials in the soma and distal axonal recording sites failed (Fig. 4*F*, *), we presume that this component represents the generation of an action potential in the axon initial segment. This IS spike was followed, in the soma, by the initiation of a somatodendritic (SD) spike. Similarly, in the distal axon (DA), local action-potential generation was also preceded by the IS spike (Fig. 4*F*).

The intracellular injection of a depolarizing current pulse into the distal axon (110–309 μ m from the soma) resulted in the initiation of single spikes only that back-propagated into the soma (Fig. 4*E*; $n = 16$). Even intense, prolonged depolarization of the distal axon failed to initiate trains of action potentials (Fig. 4*E*), a property previously reported for axons and that appears to result from a high density of low-threshold K⁺ channels in the axon (Dodson et al. 2003; Waxman 1995). As mentioned in the preceding text, prolonged depolarization of the proximal axon (22–97 μ m from the soma; $n = 6$) resulted in repetitive spike discharge, similar to that seen with somatic depolarization (not shown). Thus the soma, proximal axon, and distal axon all exhibited distinct electrophysiological features.

Properties of myelination of axons in ferret prefrontal cortex

Previous reports have compared the site of spike initiation with the pattern of myelination to demonstrate that spikes are initiated either in the axon initial segment or the first node of Ranvier (Clark et al. 2005; Palmer and Stuart 2006). Here we also compared the pattern of myelination in layer 5 pyramidal neurons in the ferret prefrontal cortex with our calculation of the spike initiation point. The initial portions of the principal axon of cortical pyramidal cells contains four components that we will consider here: the axon hillock, which is characterized by the initial tapered component of the axon at its origin (typically the cell body but on occasion a dendrite); the axon initial segment; the myelinated segment of the axon; and the first node after myelination. To determine these components in layer 5 cortical pyramidal cells of the ferret prefrontal cortex, we examined the myelination of these axons through both Golgi-stained material (Fig. 5*B*) as well as immunofluorescence staining against myelin on neurons that were also filled with biocytin and Alexa-488 (Fig. 5, *C* and *D*; supplementary Fig. 2).

First, we examined the overall pattern of myelination of the 7-wk-old ferret prefrontal cortex through silver-stain visualization of myelin (Fig. 5*A*; METHODS). This method revealed dark staining only within the white matter, with relatively little staining in the medial or lateral banks of the prefrontal cortex

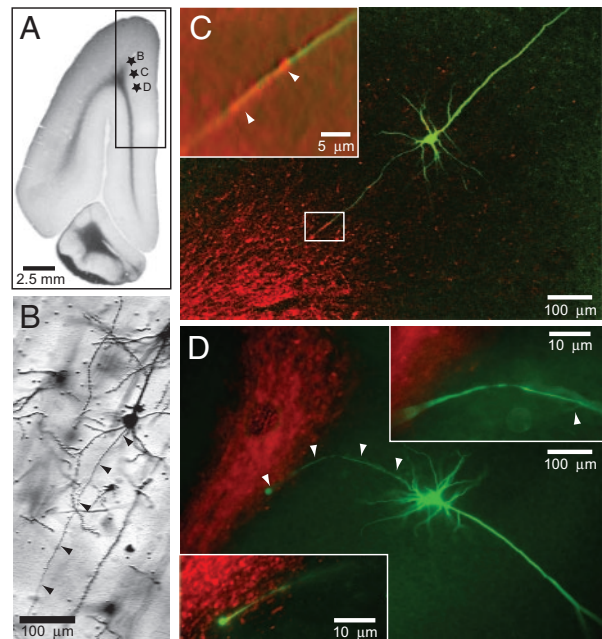


FIG. 5. Axons of layer 5 pyramidal cells of the ferret prefrontal cortex are unmyelinated for a prolonged distance. *A*: silver staining of myelin (dark areas) in the 7-wk-old ferret prefrontal cortex shows little or no myelin present within the gray matter (light areas). *B*: Golgi staining, which does not stain myelinated axons, confirms that axons of layer 5 pyramidal cells are unmyelinated for prolonged (>100 μ m) distances in this 7-wk-old animal (see also supplementary Fig. 2). *C* and *D*: intracellularly labeled prefrontal layer 5 pyramidal cells (green) double labeled for the presence of myelin (red) using immunohistochemistry. Myelination starts as the axon enters the corpus callosum (*C*), although in the large majority of in vitro cases ($n = 12/15$) the axon is cut before myelination starts (*D*). *C*, inset: arrows, the beginning of the myelin sheath in the single labeled axon. *D*: arrows, main axon shaft; top right inset: arrow, axon collateral.

(Fig. 5*A*; $n = 6$ ferrets). In contrast, silver-stain based visualization of myelination in the primary visual cortex from the same animals revealed typical bands of myelin in both the white matter as well as within layers 4 and 5 (not shown).

To examine the issue of myelination of layer 5 pyramidal cell axons in the ferret prefrontal cortex further, we examined Golgi-stained material (see METHODS). Golgi staining reveals axons only if they are unmyelinated (Fairen et al. 1977). Therefore the point at which axons emanating from the cell body lose Golgi staining should indicate the approximate beginning of myelination. Examination of Golgi stained sections revealed that in the 7-wk-old ferret prefrontal cortex the principal axon extends for a long distance (average of 212 ± 118 μ m; $n = 38$) from the soma before staining is lost. Examination of Golgi-stained material from the prefrontal cortex of older ferrets (15 mo) revealed that these also appear to be unmyelinated for a long distance (138 ± 103 μ m; $n = 46$) although this distance is less than in 7-wk-old animals. The long length of axon that is visualizable with Golgi staining in the ferret prefrontal cortex is in contrast to that previously reported for many neocortical pyramidal cells (Farinas and DeFelipe 1991). Indeed, when we examined Golgi-stained layer 5 pyramidal cells in the ferret primary visual cortex, the axons became unlabeled at a much shorter distance (36 ± 19 μ m in 7 wk old; $n = 30$; 54 ± 46 μ m in 15 mo old; $n = 30$; supplementary Fig. 2).

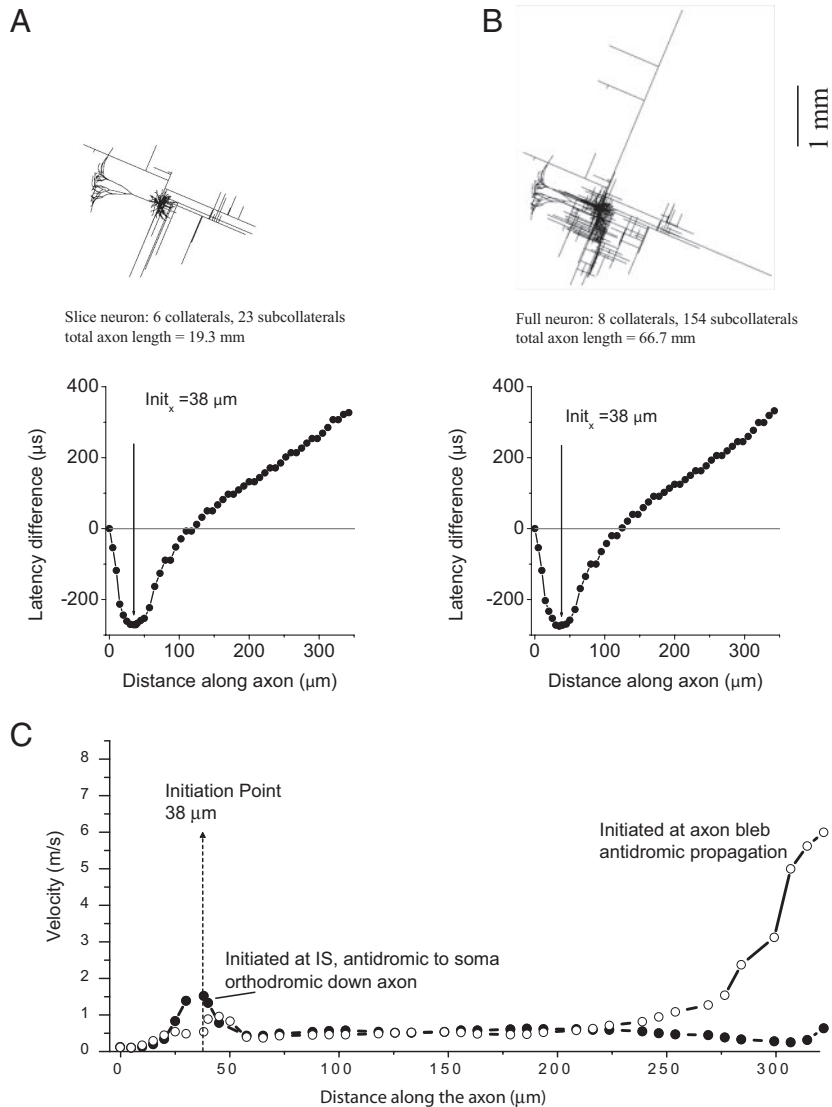


FIG. 6. Computational model of spike initiation in a layer 5 cortical pyramidal cell. *A*: computational model of a layer 5 regular spiking pyramidal cell that has the amount of axon that is typical of these neurons *in vitro* (Shu et al. 2006). The timing difference in the peak of the action potential (soma–axon) is plotted against the distance along the axon from its point of origin (edge of the cell body). The initiation point is in the region near 38 μm from the soma. *B*: action-potential initiation in the model of the layer 5 pyramidal cell with its full axon intact. Again, the initiation point is at $\sim 38 \mu\text{m}$ from the cell body. *C*: calculation of the local velocity of action-potential propagation either when the action potential is initiated with an intrasomatic current pulse (●) or with a current pulse delivered at 300 μm down the axon (○). Depolarization of the end of the axon results in rapid propagation of spikes in this region, and we calculate that differences in the orthodromic and antidiromic propagation speeds result in an 8- μm mismatch between the estimated and actual location of action-potential initiation.

To examine the location of myelination more directly, we performed immunofluorescent staining of myelin basic protein (MBP) on prefrontal cortical layer 5 neurons that had been previously filled with biocytin and a fluorescent dye (Alexa 488; 7-wk-old ferrets). Of 15 neurons examined, the axons of 12 were cut at the surface of the slice at an average distance of $289 \pm 144 \mu\text{m}$ before myelination became evident. The axons of the three remaining cells became myelinated at an average distance of $453 \pm 87 \mu\text{m}$, corresponding roughly with the location of their entry into the white matter (Fig. 5, *C* and *D*). These results indicate that in layer 5 pyramidal neurons of the ferret prefrontal cortex, action potentials are initiated in the initial, unmyelinated portion of the axon and that this location does not correspond to the beginning of myelination as it does in some preparations (Palmer and Stuart 2006).

Location of first axon collateral

The first axon collateral is often associated with the first node of Ranvier (Fraher and Kaar 1984; Sloper and Powell 1979), which has been suggested to be the location of action-potential generation in some cell types (Clark et al. 2005;

Colbert and Johnston 1996; Coombs et al. 1957). Here we examined the distance from the cell body to the first axon collateral in Golgi-stained sections of ferret prefrontal cortex. Of 38 cells examined in 7-wk-old ferrets, 26 exhibited at least one axon collateral, and the average distance to the first collateral from the soma was $104.3 \pm 32.1 \mu\text{m}$. This distance is similar to that obtained by examining the distance to the first axon collateral in biocytin/Alexa-488-filled pyramidal cells (112.5 ± 25.7 ; $n = 14$). In adult (15 mo old) ferrets, the distance to the first axon collateral in Golgi-stained sections was similar ($105 \pm 26 \mu\text{m}$; $n = 10$). Thus the calculated location of action-potential initiation is significantly proximal to the location of the first axon collaterals in our layer 5 pyramidal neurons.

Computational model of action-potential initiation and propagation

One possible modifying factor in calculating the location of spike initiation is the assumption that orthodromic and antidiromic spikes propagate at the same velocity from their site of origin. We examined this using computational models of either

a restricted, “slice-like” axonal arbor, or a complete arbor (Mainen and Sejnowski 1996; Mainen et al. 1995; Shu et al. 2006). In both the partial and complete axonal arbor models, spikes initiated at 38 μm from the root of the axon in response to somatic current injection (Fig. 6). Increasing the axonal density of gNa^+ , starting with levels equal to that of the soma, moved the action-potential initiation point along the axon away from the soma. This progression down the axon exhibited a plateau of $\sim 40 \mu\text{m}$ (not shown). In our model of axonal action-potential generation, the spikes were found to propagate orthodromically down the axon and antidromically toward the cell body at different rates (Fig. 6C). In simulations in which the main axon terminated at lengths similar to those in our actual recordings, we calculated that this difference in orthodromic and antidromic propagation velocity will cause the calculated point of initiation in real recordings to be on average $\sim 10 \mu\text{m}$ farther down the axon than the actual initiation point. Including this correction factor results in an estimated initiation point of between 30 and 45 μm from the soma in our recordings from real neurons.

Using current pulses to initiate action potentials at the cut end of the axon can also result in a miscalculation of the point of initiation of action potentials. This is because the spikes recorded at, for example, 300 μm from the soma propagate at different velocities according to whether they are initiated locally and propagate antidromically or initiated at the axon initial segment and propagate orthodromically (Fig. 6C). Antidromic spikes propagate more quickly at their site of initiation (300 μm from the soma in this model), owing to the depolarization of the axon by the current pulse during antidromic activation. In contrast, initiation of spikes with somatic current pulse did not result in such a large effect at the site of spike initiation (axon initial segment). The differences in average propagation velocity suggest that our algebraic calculations from the data obtained in real neurons (Fig. 3) may estimate the location of spike initiation to be distal to the actual site of spike initiation by $\sim 8 \mu\text{m}$, resulting in a corrected location of $\sim 38 \mu\text{m}$ from the soma.

Spike threshold varies with distance from the soma

To examine the possibility that the axon initial segment has a lower threshold for action-potential initiation, we plotted the membrane potential at which spikes were initiated with intraxonal current pulses versus distance along the axon from the soma (Fig. 7). This plot revealed a relationship in which the threshold increased with distance down the axon, after a distance of $\sim 100 \mu\text{m}$ (Fig. 7; $n = 20$ axonal recordings). Plotting the best linear fit for all points distal to 50 μm and the best linear fit for points $\leq 75 \mu\text{m}$ revealed an intersection at $\sim 60 \mu\text{m}$. Although there is considerable variation in this plot of spike threshold (each point represents a different cell), the data suggest that the axonal region up to $\sim 100 \mu\text{m}$ from the soma has a lower spike threshold than the more distal axon.

Spikes occurring *in vivo* have initiation properties suggestive of an axonal origin

Recently we have demonstrated that somatic recordings of action potentials that originate in the axon reveal an unusually rapid rate of rise at the foot of the spike (McCormick et al.

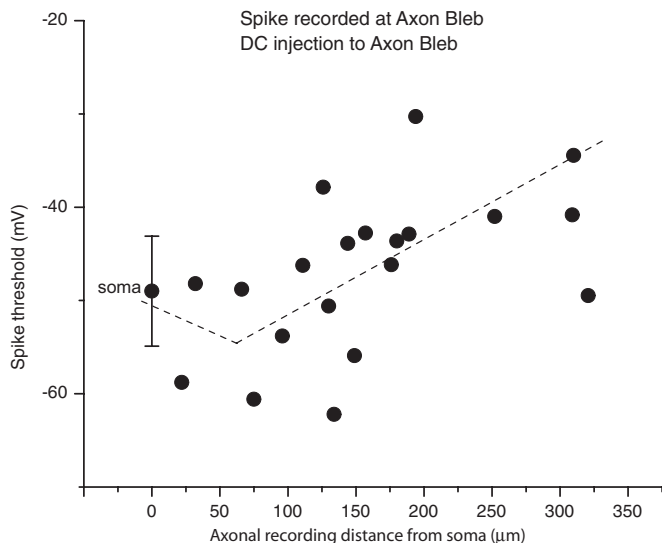


FIG. 7. Relationship between spike threshold and distance along the axon. The membrane potential at which the 1st spike was initiated in response to the injection of a depolarizing current pulse was measured at the soma (1st point with SE bars) and at varying distances along the axon. Each point represents a single neuron. The threshold for activation of an action potential is lower in the proximal 100 μm of the axon than in the more distal 200 μm of axon. There is a rough relationship between distance and threshold (---), which is consistent with initiation of action potentials within the 1st 100 μm of the axon. Action-potential threshold was defined as the membrane potential at which dV/dt passed 25 V/s.

2006), giving rise to the so-called action-potential “kink” (Naundorf et al. 2006). Here we examined whether or not this was also true for action potentials that were initiated in the apical dendrite of layer 5 pyramidal cells (Fig. 8). Through the intracellular injection of large (0.8–2 nA; 100–500 ms) current pulses into the proximal to middle (150–420 μm) portions of the apical dendrite, we were able to cause the dendritic initiation of fast action potentials that then propagated to the soma. Examination of these somatic spikes revealed a relatively slow, or smooth, transition at the initiation point of the spike (Fig. 8A; $n = 105$ spikes in 4 cells). In contrast, examination of somatic action potentials generated in response to somatic current injection and that were known, from dual somatic/axonal whole cell recordings, to have originated in the axon exhibited a prominent kink at spike initiation (Fig. 8B; $n = 2671$ spikes in 13 cells). Plotting the slope of the phase plot at spike initiation for action potentials known to be initiated in the axon or the apical dendrite revealed very distinct distributions (Fig. 8E). Next we compared the distributions of the slopes at spike initiation of action potentials occurring *in vivo* during either up states in the prefrontal cortex of the ferret (Haider et al. 2006) or during visual stimulation in the cat primary visual cortex (Fig. 8E) (Nowak et al. 2005). Interestingly, both spikes initiated during up states in the ferret prefrontal cortex ($n = 2364$ spikes in 11 cells) and spikes initiated by visual stimuli in the cat primary visual cortex exhibited a prominent kink at spike onset (Fig. 8C; $n = 4,298$ spikes in 10 cells). This result was quantified by measuring the slope of the phase plot of spike dV/dt versus membrane potential (Naundorf et al. 2006; McCormick et al. 2006) (Fig. 8D). The distributions of the slope of the phase plot at spike initiation for *in vivo* spikes during up states as well as visually evoked spikes were very

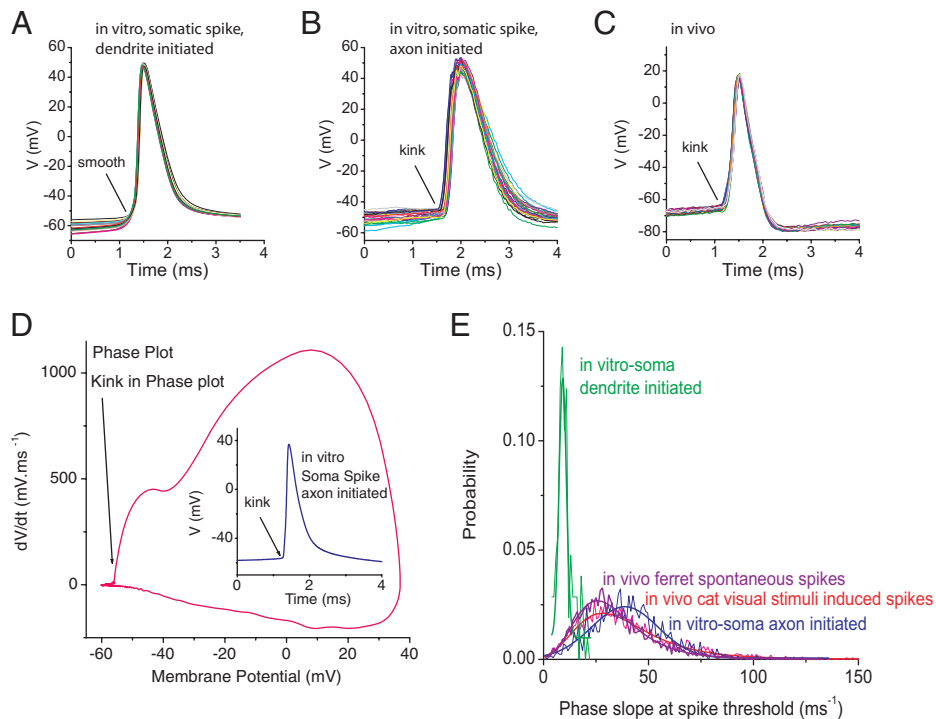


FIG. 8. Spikes occurring *in vivo* have properties consistent with initiation in the axon. *A*: overlay of action potentials recorded *in vitro* in the soma of layer 5 pyramidal cells after their initiation through the delivery of a large current pulse in the apical dendrite (280 μm from the soma). Note the smooth rise at the foot of the action potential. *B*: action potentials that initiate in the axon (as revealed by simultaneous axonal and somatic whole cell recordings) exhibit a prominent “kink” at the initiation point. *C*: action potentials recorded in the cat primary visual cortex *in vivo* during visual stimulation also exhibit a prominent kink. *D*: phase plot of the dV/dt vs. membrane potential for an action potential that initiates in the axon shows a rapid slope at the initiation point of the spike (raw spike is shown in *inset*). *E*: histograms of the distribution of the slopes of the phase plots (at $dV/dt = 15$ mV/ms) for spikes initiated in the axon (blue), initiated in the apical dendrite (green) and as recorded *in vivo* in the cat primary visual cortex during visual stimulation (red) or *in vivo* in the ferret prefrontal cortex during the generation of up states (purple). Note the similarity between the distributions recorded *in vivo* and the spikes initiated in the axon *in vitro*. Slopes were measured as the average slopes of 3 adjacent points in the phase plot of dV/dt vs. V_m at the criteria level of 15 mV/ms for each action potential.

similar to that for *in vitro* somatic recordings of axonally initiated spikes in layer 5 pyramidal cells (Fig. 8*E*). In contrast, the distributions of *in vivo* spike phase plot slopes were completely different from those for spikes known to have originated in the apical dendrite *in vitro* (Fig. 8*E*). These results indicate that spikes occurring in cortical neurons *in vivo*, either during spontaneous up states in anesthetized ferrets or during visual stimulation in anesthetized cats, are primarily initiated in the axon.

Properties of axonal spike initiation during epileptiform activity

Previous studies have suggested that dendritic spike initiation may occur when the dendrites are strongly and/or synchronously depolarized (Golding and Spruston 1998; Kloosterman et al. 2001; Stuart et al. 1997b; Turner et al. 1991). In addition, the pattern and properties of spike generation in axons may be very important in the generation of epileptiform activity (Meeks et al. 2005; Noebels and Prince 1978). Here we examined the point of initiation of fast action potentials during the generation of epileptiform activity in prefrontal cortical slices. After the bath application of 50 μM picrotoxin, and in the presence of 1 mM Mg^{2+} and 1 mM Ca^{2+} (Sanchez-Vives and McCormick 2000; Shu et al. 2003a,b), cortical slices generated prolonged (0.4–8 s) epileptiform bursts consisting of an initial large depolarization and inactivation of somatic spikes, followed by repetitive bursts of action potentials (Fig. 9). This epileptiform activity is known to be generated through recurrent excitatory networks within the cortical slice and is associated with very strong barrages of excitatory and inhibitory (although GABA_A receptors are blocked here) synaptic activity (reviewed in McCormick and Contreras 2001).

Simultaneous somatic and apical dendritic (50–90 μm from the soma) recordings during the generation of epileptiform activity revealed that each fast action potential occurred in the

soma prior to the apical dendrite (Fig. 9*A*). We failed to observe any spikes that exhibited an onset in the proximal apical dendrite prior to the soma, indicating that even under this situation of strong dendritic depolarization, fast spikes still are back-propagating between the soma and proximal apical dendrite. To examine if these spikes were initiated in the axon initial segment, we performed whole cell recordings from axons that were relatively short in length (50–77 μm ; $n = 6$), with the hypothesis that action potentials initiated in the axon would occur first at these short axonal distances in comparison to the soma. Indeed, these dual somatic/axonal recordings demonstrated that during the generation of epileptiform activity, all action potentials, whether they were in the initial, or subsequent, bursts, exhibited an earlier onset in the proximal axon than in the soma (Fig. 9*B*). The timing difference between the axon and the soma was consistent with axonal initiation at ~45 μm from the soma of these epileptiform spikes (Fig. 1*G*).

Simultaneous whole cell recording from the soma and proximal to distal parts of the axon (60–300 μm) during epileptiform activity demonstrated that these portions of the axon followed action-potential generation in the soma on a nearly one to one fashion with failures of spike initiation and conduction being rare (Figs. 9 and 10; $n = 6$). The large depolarization (paroxysmal depolarization shift, PDS) associated with epileptiform bursts was also present in the axon, although the amplitude of this decreased with distance from the soma (Figs. 9 and 10). The large depolarizations, particularly the first PDS, associated with epileptiform activity could strongly reduce the amplitude of spikes generated in the soma and, to some degree, in the axon initial segment (Fig. 10). However, the number of action potentials generated in the proximal and distal axon during the initial PDS was often greater than in the soma (Figs. 9, *C* and *D*, and 10*B*).

Previously, simultaneous somatic whole cell and axonal extracellular recordings suggested that cortical axons do not

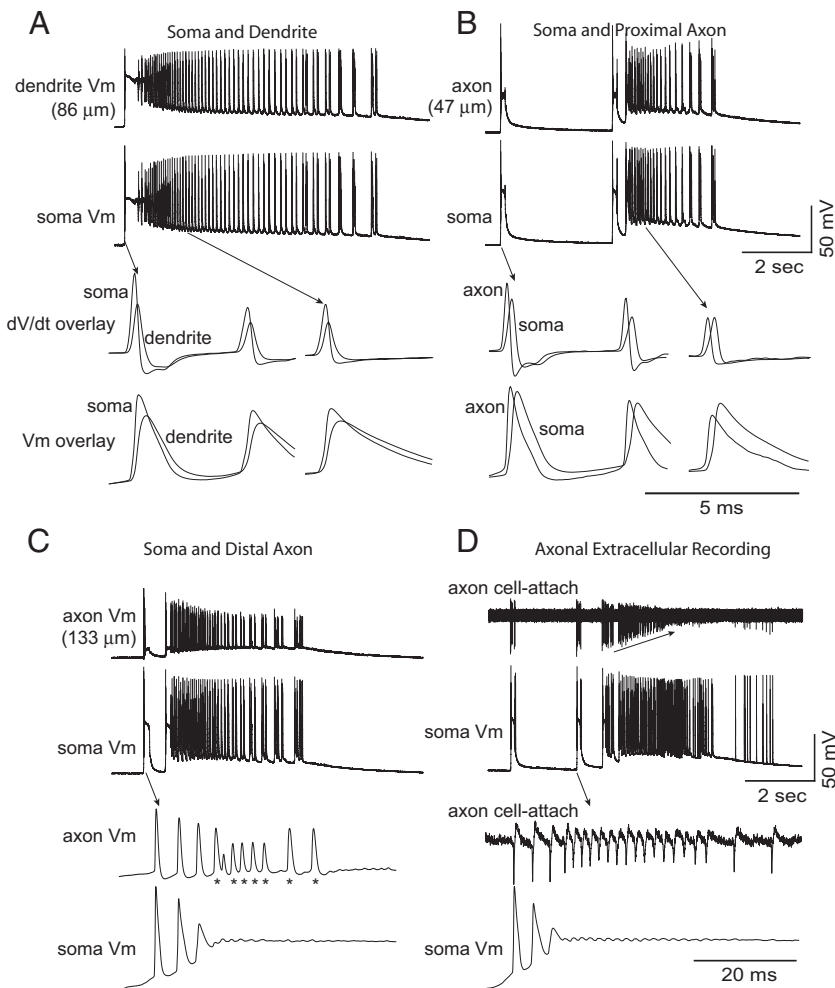


FIG. 9. Spikes are initiated in the axon and propagate through the cell and apical dendrite during epileptiform activity. *A*: simultaneous whole cell and dendritic (86 μ m) recording during the generation of epileptiform activity induced by the block of GABA_A ionophores with the bath application of picrotoxin (50 μ M). *B*: simultaneous whole cell recording from the soma and axon (47 μ m from the soma) during the generation of epileptiform activity. *C*: simultaneous whole cell recording from the cell body and more distal axon (133 μ m) during the generation of epileptiform activity. Note that the more distal axon generates several spikes during the initial paroxysmal depolarization shift that do not occur in the soma. *D*: simultaneous whole cell somatic and extracellular axonal recording, demonstrating that during epileptiform bursts, axonal spikes may become smaller than background noise levels in extracellular recordings. Same cell as recorded in *C*.

faithfully follow or generate epileptiform bursts as well as pyramidal cell bodies (Meeks et al. 2005); this is in direct contrast to our results here. To test the possibility that this discrepancy may result from differences in the recording techniques, we recorded extracellularly (as per Meeks et al. 2005) from the same axons that we had previously performed whole cell recordings and compared the results. We found that axonal action potentials recorded extracellularly could suffer from a significant signal to noise problem. Many of the spikes that were previously observed with axonal whole cell recording disappeared into the background noise of the recording when recorded extracellularly (cf. Fig. 9, *C* and *D*).

DISCUSSION

Cortical neurons *in vivo* undergo a constant bombardment of synaptic activity arriving throughout the soma, dendrites, and axon initial segment. Detailed *in vitro* investigations indicate that each of these compartments of the neuron are capable of generating action potentials and simultaneous whole cell recordings from the soma and apical dendrites or soma and even distal axons (Shu et al. 2006) indicate that this ongoing synaptic activity can propagate long distances (>0.5 mm) along these processes. Which compartment then will initiate the fast action potentials that propagate down the axon in response to this synaptic bombardment?

Prior *in vitro* studies suggest that fast action-potential initiation will most often occur in the axon in pyramidal cells, followed by back propagation into the somatic and dendritic compartments (Stuart et al. 1997a,b). However, exactly which compartment of the axon will initiate the action potential has been an open question, with studies favoring both the axon initial segment (Palmer and Stuart 2006; Stuart et al. 1997a) as well as the first node of Ranvier (Clark et al. 2005; Colbert and Johnston 1996; Colbert and Pan 2002). A recent imaging study using voltage-sensitive dye indicates that action potentials initiated in response to current pulses and single excitatory postsynaptic potentials (EPSPs) evoked with local electrical stimulation occur first ~ 35 μ m down the main axon from the soma (Palmer and Stuart 2006). To put this in perspective, it is worth reviewing the structure of cortical axons. Axons from pyramidal neurons typically arise from the cell body, although they can also emanate from a basal dendrite (Palay et al. 1968). The transition between the axon and the soma/dendrite from which it originates is associated with a conical, ~ 5 μ m long, transition segment, the axon hillock. The axon initial segment follows the axon hillock. It is typically a 17- to 40- μ m long segment of axon that on the electron microscopic level contains a layer of dense granular material underneath the membrane, microtubules in the cytoplasm, and scattered clusters of ribosomes (Farinas and DeFelipe

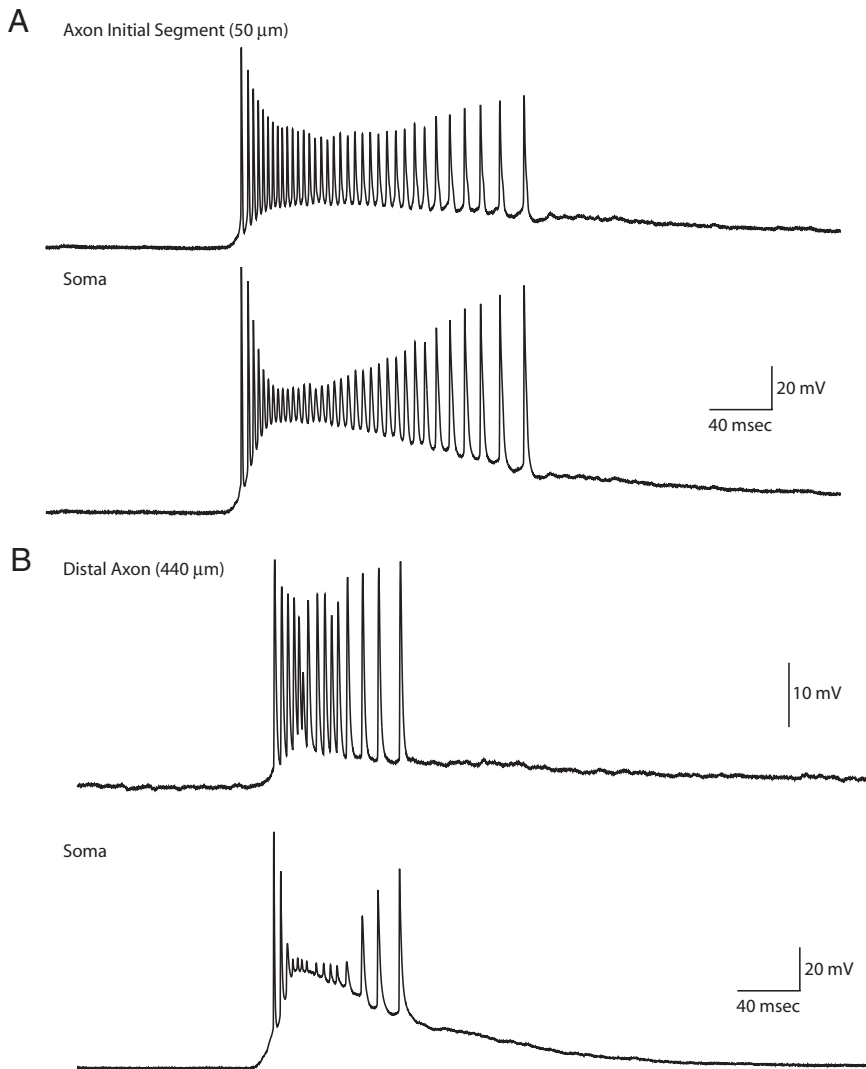


FIG. 10. Action potentials maintain their height in the distal axon better than the proximal axon and soma during epileptiform activity. **A:** simultaneous recording of an epileptiform burst in the soma and axon (50 μm from the soma). Note that during the epileptiform burst spikes decrease dramatically in amplitude in the soma but also decrease to some degree in the axon initial segment. **B:** simultaneous recording of an epileptiform burst in the soma and distal axon (440 μm from the soma). Note that although the amplitude of spikes in the soma is dramatically affected by the epileptiform burst, the amplitude of spikes in the distal axon is not strongly affected.

1991; Inda et al. 2006; Palay et al. 1968). Immunocytochemical localization of Na^+ channels, K^+ channels, and cytoskeleton and adhesion molecules spectrin β IV and Caspr2 reveal a high density in the axon initial segment (as well as at nodes of Ranvier) (Inda et al. 2006). Often, but not always, the end of the axon initial segment (as defined by the loss of the submembranous structures typical of the initial segment on the EM level) is associated with the beginning of myelination (Farinas and DeFelipe 1991; Palay et al. 1968). In the layer 5 neurons studied here, the main axons were unmyelinated for approximately $\geq 200 \mu\text{m}$ (see Fig. 5, supplementary Fig. 2). Our results indicate that action potentials typically initiate in a region that is $\sim 35\text{--}50 \mu\text{m}$ from the soma, long before the axons are myelinated in these cells. Although Palmer and Stuart (2006) have suggested that the action-potential initiation site corresponds to the beginning of myelination, these authors also observed a proximal initiation site at early postnatal ages when axons are unmyelinated. Together, these and our results suggest that the region of myelination by itself does not determine the site of spike initiation. Immunocytochemical studies suggest that the axon initial segment may contain a high density of Na^+ and K^+ channels, causing it to have a low

threshold for action-potential initiation (Inda et al. 2006; Komada and Soriano 2002). Our high-resolution recordings of action potentials in the axon initial segment reveal a very high rate of rise for these spikes, indicating a relatively high local density of Na^+ channels (McCormick et al. 2006). In contrast, direct recordings of Na^+ and K^+ channels from the initial segment suggest an alternative interpretation. The Na^+ channels at the axon initial segment may have a more negative activation curve than those in the soma (Colbert and Pan 2002). In addition to the presence of a high density of Na^+ channels, and/or the presence of Na^+ with low threshold, the electrical characteristics of the axon initial segment are conducive to the initiation of action potentials. The large capacitive and conductance load of the soma and dendrites decreases with increased distance down the axon, thereby decreasing the amount of current required to initiate an action potential. As synaptic activity arriving in the dendrites and soma of the neuron propagates down the axon (Alle and Geiger 2006; Shu et al. 2006), the axon initial segment forms the location that is most favorable to action-potential initiation. This region of the cell is strongly affected by the summed membrane potential arriving from the various dendritic branches and soma (Shu et al. 2006) and its electrical properties (e.g., channel densities and properties,

electrical isolation, etc.) facilitate the production of action potentials.

Where do action potentials initiate *in vivo*? This is a difficult question to answer because simultaneous recordings with high temporal resolution from different portions of pyramidal cells, which also include the axon, *in vivo* are not yet possible. Prior extracellular recording studies indicate that action potentials typically are back propagating from the soma into the apical dendrites (Buzsaki and Kandel 1998), indicating that the spikes initiated somewhere within the soma, basal dendrites, or axon compartments. One property of action potentials offers an interesting possibility to decipher the region of origin of action potentials *in vivo*. Recently it was noted that spikes occurring in cortical neurons exhibit a prominent and characteristic rapid rate of rise at their initiation, giving rise to a so-called “kink” (Naundorf et al. 2006) (Fig. 8). Detailed recordings and simulations of cortical pyramidal cells reveal that this kink in the action potential arises from spike initiation in the axon (McCormick et al. 2006), owing in part to the high density of Na^+ channels apparently present in the axon initial segment (Inda et al. 2006; Komada and Soriano 2002). Our recordings reveal that spikes initiated in the apical dendrite do not share this property of axonally initiated action potentials (see Fig. 8). When we examined the properties of spikes occurring *in vivo*, during either spontaneous up states in anesthetized ferrets or visual stimulation in anesthetized cats, we found a distribution of rate of rise at the foot of the spike that was very similar to spikes initiated in the axon in layer 5 pyramidal neurons *in vitro*. The strong overlap in these distributions suggests that spikes that we recorded *in vivo* were preferentially initiated in the axon. The small difference in spike slope distributions (see Fig. 8) between *in vivo* and *in vitro* suggests that a small percentage of spikes *in vivo* may have originated in the dendrites. However, it is also possible that these differences arise from comparing the spikes of different cell types (e.g., layer 5 pyramids *in vitro* versus multiple cell types *in vivo*) or differences in important physiological parameters between *in vivo* and *in vitro* (e.g., modulators, ion concentrations, anesthetics, etc.).

Prior studies have suggested that strong depolarization of dendritic compartments may give rise to local spike initiation that then propagates to the soma/axon initial segment (Gasparini et al. 2004; Golding and Spruston 1998; Larkum and Zhu 2002; Larkum et al. 1999a,b 2001; Losonczy and Magee 2006; Milojkovic et al. 2005; Regehr et al. 1993; Schiller et al. 1997). Given this, one might expect that epileptiform discharges, which are mediated by very strong excitatory synaptic barrages arriving in pyramidal cell dendrites, would be associated with dendritic action-potential initiation. Perhaps surprisingly, we found that during epileptiform activity after disinhibition *in vitro*, fast action potentials were always initiated in the axon initial segment, followed by back-propagation into the soma and apical dendrite. Presumably, this axonal site of initiation results from the arrival of large barrages of EPSPs in the basal dendrites, which are electronically closer to the axon initial segment than the distal apical dendrite. Indeed, cortical pyramidal cells receive $\sim 75\text{--}95\%$ of their excitatory synaptic (spinous) inputs in the basal and nearby oblique apical dendrites in the neocortex, within $\sim 200\ \mu\text{m}$ from the soma (Larkman 1991), indicating that the distal apical dendrite may form a relatively minor, but unique, source of excitatory input

to these cells. Voltage-sensitive dye imaging of action potentials generated in pyramidal cells in response to somatic current injection or local applications of glutamate to the basal dendrites indicate that these spikes typically back-propagate from the soma into the basal dendrites (Kampa and Stuart 2006; Milojkovic et al. 2005). In a minority of cells, fast prepotentials (spikelets) originating in the basal dendrites were observed to precede spike initiation in the soma/axon (Milojkovic et al. 2005). Although we did not observe these spikelets in our *in vitro* or *in vivo* recordings, spikelets (termed fast prepotentials) have been observed in a minority of other intracellular recordings *in vivo* (Crochet et al. 2004). However, there are multiple possible sources for these spikelets other than action-potential generation in the basal dendrites, including action-potential generation in other neurons that are coupled to the recorded cell either through gap junctions or artificially through a “double impalement” with the intracellular electrode or distal axonal spike initiation. Thus spikelets are relatively rare events and their occurrence is not restricted to spike initiation in the basal dendrites.

Do all fast action potentials initiate in the axon initial segment? We do not deny the existence of action potentials that are initiated in isolated dendritic locations nor the possible occurrence of action potentials that propagate forward to the soma and axon initial segment and result in the initiation of spike discharge (for example, the generation of intrinsic bursts is likely to result in part from the prolonged depolarization of the soma by active conductances in the dendrite). Rather, our data emphasize the strong and dominant influence of the axon initial segment in the initiation of fast action potentials in cortical layer 5 pyramidal cells during periods of relatively moderate frequency, synaptically driven activity as well as during epileptiform bursts. Prior *in vitro* studies have repeatedly demonstrated the ability of particular patterns or locations of dendritic inputs to initiate action potentials in local dendritic branches that may or may not initiate spikes in the axonal/somatic compartments (Gasparini et al. 2004; Golding and Spruston 1998; Kampa and Stuart 2006; Larkum and Zhu 2002; Larkum et al. 1999a,b, 2001; Losonczy and Magee 2006; Milojkovic et al. 2005; Polsky et al. 2004; Regehr et al. 1993; Schiller et al. 1997; Wei et al. 2001). Our present studies do not rule out the occurrence of dendritic action potentials, especially in the distal apical tuft or distal basal dendrites, that failed to propagate to the portions of the neuron from which we recorded (main shaft of the apical dendrite, soma, axon).

Even if all or nearly all fast spikes are initiated in the axon initial segment, the generation of regenerative potentials in the dendrites (e.g., spikes) can significantly modulate the overall pattern of discharge. For example, intrinsic burst generation in cortical neurons can result from the interaction of fast spike initiation in the axon modulated by the occurrence of slower Na^+ - and/or Ca^{2+} -mediated spikes in the dendrites that are initiated either by synaptic input or through interactions with the back propagating spikes from the axon/soma (Helmchen et al. 1999; Kim and Connors 1993; Larkum and Zhu 2002; Larkum et al. 2001; Stuart et al. 1997b; Wang 1999) and the activation of dendritic spikes can significantly alter the timing of spike initiation in the axon/somatic region (Ariav et al. 2003).

The precise pattern of spike generation within neurons undergoing synaptic barrages in various behavioral circumstances *in vivo* will be complex with interactions between all of

the different compartments of each cortical neuron. Our present results indicate that under a variety of naturalistic situations, the axon initial segment is the preferred site of fast spike initiation in cortical pyramidal cells. Further investigations are required before the full complexity of spike initiation and propagation in cortical neurons will be understood.

ACKNOWLEDGMENTS

Present address of Y. Shu: Lab of Neural Network Function, Institute of Neuroscience, Chinese Academy of Sciences, 320 Yueyang Road, Shanghai 200031, China.

GRANTS

This work was supported by the National Institutes of Health and the Kavli Institute for Neuroscience to D. A. McCormick.

REFERENCES

- Alle H, Geiger JR.** Combined analog and action potential coding in hippocampal mossy fibers. *Science* 311: 1290–1293, 2006.
- Ariav G, Polsky A, Schiller J.** Submillisecond precision of the input-output transformation function mediated by fast sodium dendritic spikes in basal dendrites of CA1 pyramidal neurons. *J Neurosci* 23: 7750–7758, 2003.
- Azouz R, Gray CM.** Cellular mechanisms contributing to response variability of cortical neurons in vivo. *J Neurosci* 19: 2209–2223, 1999.
- Binzegger T, Douglas RJ, Martin KA.** Axons in cat visual cortex are topologically self-similar. *Cereb Cortex* 15: 152–165, 2005.
- Buzsaki G, Kandel A.** Somadendritic backpropagation of action potentials in cortical pyramidal cells of the awake rat. *J Neurophysiol* 79: 1587–1591, 1998.
- Clark BA, Monsivais P, Branco T, London M, Häusser M.** The site of action potential initiation in cerebellar Purkinje neurons. *Nat Neurosci* 8: 137–139, 2005.
- Colbert CM, Johnston D.** Axonal action-potential initiation and Na^+ channel densities in the soma and axon initial segment of subiculum pyramidal neurons. *J Neurosci* 16: 6676–6686, 1996.
- Colbert CM, Pan E.** Ion channel properties underlying axonal action potential initiation in pyramidal neurons. *Nat Neurosci* 5: 533–538, 2002.
- Coombs JS, Curtis DR, Eccles JC.** The interpretation of spike potentials of motoneurons. *J Physiol* 139: 198–231, 1957.
- Crochet S, Fuentealba P, Timofeev I, Steriade M.** Selective amplification of neocortical neuronal output by fast prepotentials in vivo. *Cereb Cortex* 14: 1110–1121, 2004.
- Destexhe A, Rudolph M, Fellous JM, Sejnowski TJ.** Fluctuating synaptic conductances recreate in-vivo-like activity in neocortical neurons. *Neuroscience* 107: 13–24, 2001.
- Dodson PD, Billups B, Rusznak Z, Szucs G, Barker MC, Forsythe ID.** Presynaptic rat Kv1.2 channels suppress synaptic terminal hyperexcitability following action potential invasion. *J Physiol* 550: 27–33, 2003.
- Fairen A, Peters A, Saldanha J.** A new procedure for examining Golgi-impregnated neurons by light and electron microscopy. *J Neurocytol* 6: 311–337, 1977.
- Farinas I, DeFelipe J.** Patterns of synaptic input on corticocortical and corticothalamic cells in the cat visual cortex. II. The axon initial segment. *J Comp Neurol* 304: 70–77, 1991.
- Fraher JP, Kaar GF.** The transitional node of Ranvier at the junction of the central and peripheral nervous systems: an ultrastructural study of its development and mature form. *J Anat* 139: 215–238, 1984.
- Fricker D, Verheugen JA, Miles R.** Cell-attached measurements of the firing threshold of rat hippocampal neurons. *J Physiol* 517: 791–804, 1999.
- Fuortes MG, Frank K, Becker MC.** Steps in the production of motoneuron spikes. *J Gen Physiol* 40: 735–752, 1957.
- Gallyas F.** Silver staining of myelin by means of physical development. *Neurol Res* 1: 203–209, 1979.
- Gasparini S, Migliore M, Magee JC.** On the initiation and propagation of dendritic spikes in CA1 pyramidal neurons. *J Neurosci* 24: 11046–11056, 2004.
- Golding NL, Staff NP, Spruston N.** Dendritic spikes as a mechanism for cooperative long-term potentiation. *Nature* 418: 326–331, 2002.
- Golding NL, Spruston N.** Dendritic sodium spikes are variable triggers of axonal action potentials in hippocampal CA1 pyramidal neurons. *Neuron* 21: 1189–1200, 1998.
- Haider B, Duque A, Hasenstaub AR, McCormick DA.** Neocortical network activity in vivo is generated through a dynamic balance of excitation and inhibition. *J Neurosci* 26: 4535–4545, 2006.
- Helmchen F, Svoboda K, Denk W, Tank DW.** In vivo dendritic calcium dynamics in deep-layer cortical pyramidal neurons. *Nat Neurosci* 2: 989–996, 1999.
- Hines ML, Carnevale NT.** The NEURON simulation environment. *Neural Comput* 9: 1179–1209, 1997.
- Inda MC, DeFelipe J, Munoz A.** Voltage-gated ion channels in the axon initial segment of human cortical pyramidal cells and their relationship with chandelier cells. *Proc Natl Acad Sci USA* 103: 2920–2925, 2006.
- Jarsky T, Roxin A, Kath WL, Spruston N.** Conditional dendritic spike propagation following distal synaptic activation of hippocampal CA1 pyramidal neurons. *Nat Neurosci* 8: 1667–1676, 2005.
- Kampa BM, Stuart GJ.** Calcium spikes in basal dendrites of layer 5 pyramidal neurons during action potential bursts. *J Neurosci* 26: 7424–7432, 2006.
- Kim HG, Connors BW.** Apical dendrites of the neocortex: correlation between sodium- and calcium-dependent spiking and pyramidal cell morphology. *J Neurosci* 13: 5301–5311, 1993.
- Kloosterman F, Peloquin P, Leung LS.** Apical and basal orthodromic population spikes in hippocampal CA1 in vivo show different origins and patterns of propagation. *J Neurophysiol* 86: 2435–2444, 2001.
- Komada M, Soriano P.** [Beta]IV-spectrin regulates sodium channel clustering through ankyrin-G at axon initial segments and nodes of Ranvier. *J Cell Biol* 156: 337–348, 2002.
- Larkman AU.** Dendritic morphology of pyramidal neurones of the visual cortex of the rat. II. Parameter correlations. *J Comp Neurol* 306: 320–331, 1991.
- Larkum ME, Kaiser KM, Sakmann B.** Calcium electrogenesis in distal apical dendrites of layer 5 pyramidal cells at a critical frequency of back-propagating action potentials. *Proc Natl Acad Sci USA* 96: 14600–14604, 1999a.
- Larkum ME, Zhu JJ.** Signaling of layer 1 and whisker-evoked Ca^{2+} and Na^+ action potentials in distal and terminal dendrites of rat neocortical pyramidal neurons in vitro and in vivo. *J Neurosci* 22: 6991–7005, 2002.
- Larkum ME, Zhu JJ, Sakmann B.** Dendritic mechanisms underlying the coupling of the dendritic with the axonal action potential initiation zone of adult rat layer 5 pyramidal neurons. *J Physiol* 533: 447–466, 2001.
- Larkum ME, Zhu JJ, Sakmann B.** A new cellular mechanism for coupling inputs arriving at different cortical layers. *Nature* 398: 338–341, 1999b.
- Losonczy A, Magee JC.** Integrative properties of radial oblique dendrites in hippocampal CA1 pyramidal neurons. *Neuron* 50: 291–307, 2006.
- Mainen ZF, Joerges J, Huguenard JR, Sejnowski TJ.** A model of spike initiation in neocortical pyramidal neurons. *Neuron* 15: 1427–1439, 1995.
- Mainen ZF, Sejnowski TJ.** Influence of dendritic structure on firing pattern in model neocortical neurons. *Nature* 382: 363–366, 1996.
- McCormick DA, Connors BW, Lighthill JW, Prince DA.** Comparative electrophysiology of pyramidal and sparsely spiny stellate neurons of the neocortex. *J Neurophysiol* 54: 782–806, 1985.
- McCormick DA, Contreras D.** On the cellular and network bases of epileptic seizures. *Annu Rev Physiol* 63: 815–846, 2001.
- McCormick DA, Shu Y, Yu Y.** Hodgkin and Huxley model—still standing? *Nature* In press.
- Meeks JP, Jiang X, Mennerick S.** Action potential fidelity during normal and epileptiform activity in paired soma-axon recordings from rat hippocampus. *J Physiol* 566: 425–441, 2005.
- Millhouse OE.** The Golgi Methods. In: *Neuroanatomical Tract-Tracing Methods*, edited by Heimer L, Robards MJ. New York: Plenum, 1981, p. 311–344.
- Milojkovic BA, Wuskell JP, Loew LM, Antic SD.** Initiation of sodium spikelets in basal dendrites of neocortical pyramidal neurons. *J Membr Biol* 208: 155–169, 2005.
- Naundorf B, Wolf F, Volgushev M.** Unique features of action potential initiation in cortical neurons. *Nature* 440: 1060–1063, 2006.
- Noebels JL, Prince DA.** Development of focal seizures in cerebral cortex: role of axon terminal bursting. *J Neurophysiol* 41: 1267–1281, 1978.
- Nowak LG, Azouz R, Sanchez-Vives MV, Gray CM, McCormick DA.** Electrophysiological classes of cat primary visual cortical neurons in vivo as revealed by quantitative analyses. *J Neurophysiol* 89: 1541–1566, 2003.
- Nowak LG, Sanchez-Vives MV, McCormick DA.** Role of synaptic and intrinsic membrane properties in short-term receptive field dynamics in cat area 17. *J Neurosci* 25: 1866–1880, 2005.

- Palay SL, Sotelo C, Peters A, Orkand PM.** The axon hillock and the initial segment. *J Cell Biol* 38: 193–201, 1968.
- Palmer LM, Stuart GJ.** Site of action potential initiation in layer 5 pyramidal neurons. *J Neurosci* 26: 1854–1863, 2006.
- Polsky A, Mel BW, Schiller J.** Computational subunits in thin dendrites of pyramidal cells. *Nat Neurosci* 7: 621–627, 2004.
- Regehr W, Kehoe JS, Ascher P, Armstrong C.** Synaptically triggered action potentials in dendrites. *Neuron* 11: 145–151, 1993.
- Sanchez-Vives MV, McCormick DA.** Cellular and network mechanisms of rhythmic recurrent activity in neocortex. *Nat Neurosci* 3: 1027–1034, 2000.
- Schiller J, Schiller Y, Stuart G, Sakmann B.** Calcium action potentials restricted to distal apical dendrites of rat neocortical pyramidal neurons. *J Physiol* 505: 605–616, 1997.
- Shu Y, Hasenstaub A, Badoual M, Bal T, McCormick DA.** Barrages of synaptic activity control the gain and sensitivity of cortical neurons. *J Neurosci* 23: 10388–10401, 2003a.
- Shu Y, Hasenstaub A, Duque A, Yu Y, McCormick DA.** Modulation of intracortical synaptic potentials by presynaptic somatic membrane potential. *Nature* 441: 761–765, 2006.
- Shu Y, Hasenstaub A, McCormick DA.** Turning on and off recurrent balanced cortical activity. *Nature* 423: 288–293, 2003b.
- Sloper JJ, Powell TP.** A study of the axon initial segment and proximal axon of neurons in the primate motor and somatic sensory cortices. *Philos Trans R Soc Lond B Biol Sci* 285: 173–197, 1979.
- Steriade M, Nuñez A, Amzica F.** A novel slow (< 1 Hz) oscillation of neocortical neurons in vivo: depolarizing and hyperpolarizing components. *J Neurosci* 13: 3252–3265, 1993.
- Steriade M, Timofeev I, Grenier F.** Natural waking and sleep states: a view from inside neocortical neurons. *J Neurophysiol* 85: 1969–1985, 2001.
- Stuart G, Schiller J, Sakmann B.** Action potential initiation and propagation in rat neocortical pyramidal neurons. *J Physiol* 505: 617–632, 1997a.
- Stuart G, Spruston N, Sakmann B, Häusser M.** Action potential initiation and backpropagation in neurons of the mammalian CNS. *Trends Neurosci* 20: 125–131, 1997b.
- Svoboda K, Denk W, Kleinfeld D, Tank DW.** In vivo dendritic calcium dynamics in neocortical pyramidal neurons. *Nature* 385: 161–165, 1997.
- Svoboda K, Helmchen F, Denk W, Tank DW.** Spread of dendritic excitation in layer 2/3 pyramidal neurons in rat barrel cortex in vivo. *Nat Neurosci* 2: 65–73, 1999.
- Turner RW, Meyers DE, Richardson TL, Barker JL.** The site for initiation of action potential discharge over the somatodendritic axis of rat hippocampal CA1 pyramidal neurons. *J Neurosci* 11: 2270–2280, 1991.
- Wang XJ.** Fast burst firing and short-term synaptic plasticity: a model of neocortical chattering neurons. *Neuroscience* 89: 347–362, 1999.
- Waters J, Helmchen F.** Boosting of action potential backpropagation by neocortical network activity in vivo. *J Neurosci* 24: 11127–11136, 2004.
- Waxman SG.** Voltage-gated ion channels in axons: localization, function, and development. In: *The Axon. Structure, Function and Pathophysiology*, edited by Waxman SG, Kocsis JD, Styrs PK. New York: Oxford, 1995, p. 218–239.
- Wei DS, Mei YA, Bagal A, Kao JP, Thompson SM, Tang CM.** Compartmentalized and binary behavior of terminal dendrites in hippocampal pyramidal neurons. *Science* 293: 2272–2275, 2001.